

Graphical evolution of spin network states

Roumen Borissov*

Physics Department, Temple University, Philadelphia, Pennsylvania 19122

(Received 21 October 1996)

The evolution of spin network states in loop quantum gravity can be defined with respect to a time variable, given by the surfaces of constant value of an auxiliary scalar field. We regulate the Hamiltonian, generating such an evolution, and evaluate its action both on edges and on vertices of the spin network states. The analytical computations are carried out completely to yield a finite, diffeomorphism-invariant result. We use techniques from the recoupling theory of colored graphs with trivalent vertices to evaluate the graphical part of the Hamiltonian action. We show that the action on edges is equivalent to a diffeomorphism transformation, while the action on vertices adds new edges and reroutes the loops through the vertices. A remaining unresolved problem is to take the square root of the infinite-dimensional matrix of the Hamiltonian constraint and to obtain the eigenspectrum of the “clock field” Hamiltonian. [S0556-2821(97)06208-5]

PACS number(s): 04.60.Ds

I. INTRODUCTION

In canonical quantum gravity the notion of evolution requires a careful definition because the translations in the time direction can be interpreted as diffeomorphism transformations [1]. To be able to talk about evolution, we can use “relational constructions.” Some physical fields can be introduced as a reference frame with respect to which the evolution can be defined [2,5,6]. In loop quantum gravity [3], Smolin and Rovelli [6,7] define a time variable by the surfaces of constant value of an auxiliary scalar field. By fixing a gauge in this construction, an infinite number of Hamiltonian constraints (one per space point) reduces to one constraint which can be interpreted as a Schrödinger equation and a Hamiltonian operator can be identified. We use the Hamiltonian obtained in this model to investigate the evolution of quantum gravitational states. In loop quantum gravity, spin network states [8–10] furnish a complete basis of quantum kinematical states.

There exists [11,12] already a well-established procedure for expressing different quantities from quantum gravity in terms of the loop variables [4]. Then operator versions of the gravitational quantities can be defined by replacing the loop variables with the corresponding operators. Thus it is relatively straightforward to introduce a loop version for the Hamiltonian operator. We use the results from [6] and [7] as a starting point for our calculations. Our purpose is to determine in detail the way the spin network states evolve under the Hamiltonian introduced in [6]. As we will see, the result of the evolution can be split into two parts. First, there is a multiplicative factor which is finite and diffeomorphism invariant. Second, the spin network states evolve topologically: The new state is a sum of terms, each term being based on the original spin network with an added extra edge of color 1. The added edge connects pairs of the original edges, meeting at a vertex. Also, some change of coloring of the

edges occurs such that the new graph is a spin network again.

The content of the paper is as follows. In Sec. II we define the Hamiltonian and regulate it to show that it has a well-defined action on the spin network states. We also introduce a modification in the way the loop operators are defined, better suited for our calculations. Technically, the action of the Hamiltonian operator can be split into analytical and graphical parts. The analytical part includes various prefactors and integrals. The graphical part expresses the topological transformations occurring in the spin networks. In Sec. III we compute the analytical action of the Hamiltonian separately on edges and on vertices. We show that to a great extent the action on edges is equivalent to diffeomorphism transformation. Using some techniques from recoupling theory of knots and links with trivalent vertices, we perform the graphical computation of the action of the Hamiltonian in Sec. IV. The result from the graphical calculation tells us whether the diffeomorphism class of the spin network or the coloring of certain edges changes. We conclude with a discussion of some open issues.

II. HAMILTONIAN OF THE THEORY

Because of the absence of external time with respect to which the evolution can be defined, we need some additional construction. As has been shown in [6], to define time we can use the physical degrees of freedom of an auxiliary field. We start by introducing a scalar field $T(x)$. To serve as a clock, this field should be monotonically increasing everywhere on the space manifold Σ .¹ Then we can use its three-surfaces of constant value $T(x) = \text{const}$ to represent the time with respect to which the evolution will be defined. The scalar “clock” field can be incorporated in the theory through the standard Klein-Gordon Lagrangian

*Present address: Center for Gravitational Physics and Geometry, The Pennsylvania State University, University Park, Pennsylvania 16802. Electronic address: borissov@phys.psu.edu

¹We use the standard notation: $g^{\mu\nu}$ and q^{ab} are, respectively, the four-metric on $\mathcal{M} = \Sigma \times R$ and the three-metric on Σ . a, b, \dots are spatial and i, j, \dots internal indices; they all run from 1 to 3.

$$\mathcal{L}_T = \frac{\mu}{2} g^{\mu\nu}(x) \sqrt{-g(x)} \partial_\mu T(x) \partial_\nu T(x). \quad (1)$$

In this expression μ plays the role of a coupling constant between the scalar field and the gravitational field. Later on, we will treat $T(x)$ as time so that, from dimensional analysis, the constant μ should have dimensions of energy density. The momentum conjugate to the field $T(x)$ will be

$$\tilde{\pi}(x) = \frac{\partial \mathcal{L}}{\partial(\partial_0 T)} = \mu q N g^{0\mu} \partial_\mu T. \quad (2)$$

Performing a Legendre transformation, we get, for the total Lagrangian,

$$\begin{aligned} \mathcal{L} = & \tilde{\pi} \partial_0 T - N \frac{\tilde{\pi}^2}{2\mu} - N \frac{\mu}{2} q^2 q^{ab} \partial_a T \partial_b T - \tilde{\pi} N^b (\partial_b T) \\ & + \mathcal{L}_{\text{gravity}}. \end{aligned} \quad (3)$$

The Euler-Lagrange equations we obtain from this Lagrangian are

$$\frac{\delta \mathcal{L}}{\delta \tilde{\pi}} = \partial_0 T - N \frac{\tilde{\pi}}{\mu} - N^b (\partial_b T) = 0 \quad (4)$$

and

$$\frac{\delta \mathcal{L}}{\delta T} = -\partial_0 \tilde{\pi} + \mu \partial_b (N \tilde{q}^{bc} \partial_c T) + \partial_b (N^b \tilde{\pi}). \quad (5)$$

At this point we impose a gauge fixing, restricting the freedom of choosing the time coordinate. The gauge we use is $\partial_a T(x) = 0$, which, because of Eq. (4), implies that

$$\partial_0 T = N \frac{\tilde{\pi}}{\mu}.$$

Thus the lapse function $N(x)$ should satisfy the relation

$$N(x) = \frac{a(t)\mu}{\tilde{\pi}(x)}, \quad (6)$$

where $a(t)$ is an arbitrary function of (the coordinate) time. For the Hamiltonian constraint, we get

$$\tilde{\mathcal{C}}(x) = \frac{\tilde{\pi}^2}{2\mu} + \tilde{\mathcal{C}}_G(x),$$

where

$$\tilde{\mathcal{C}}_G(x) = \epsilon_{ijk} \tilde{E}^{ai} \tilde{E}^{bj} F_{ab}^k - \Lambda q = \mathcal{C}_{\text{Einstein}} - \Lambda q$$

is the gravitational Hamiltonian constraint in terms of the Ashtekar variables and Λ is the cosmological constant. According to the general prescription for gauge fixing in constraint systems, we have to compute the Poisson brackets between the gauge and existing constraints to check for secondary constraints. Thus we get

$$\{\tilde{\mathcal{C}}(x'), \partial_a T(x)\} = \partial_a \left\{ \frac{\tilde{\pi}^2(x')}{2\mu}, T(x) \right\} = \partial_a \left[\frac{\tilde{\pi}(x')}{\mu} \delta^3(x', x) \right].$$

The above expression vanishes when we smear the Hamiltonian constraint $\tilde{\mathcal{C}}(x')$ using $N(x)$ from Eq. (6). Thus the only constraint which remains to be imposed on the wave functionals of the theory is the integral of the Hamiltonian constraint with the lapse function:

$$\begin{aligned} \int_\Sigma d^3x N(x) \tilde{\mathcal{C}}(x) = & a(t)\mu \int_\Sigma \frac{d^3x}{\tilde{\pi}(x)} \left(\frac{\tilde{\pi}(x)}{\sqrt{2\mu}} + \sqrt{-\tilde{\mathcal{C}}_G(x)} \right) \\ & \times \left(\frac{\tilde{\pi}(x)}{\sqrt{2\mu}} - \sqrt{-\tilde{\mathcal{C}}_G(x)} \right) \equiv 0. \end{aligned}$$

Because we are going to impose this integral as a constraint operator, we can think of $\tilde{\pi}(x)$ as being equal to $\sqrt{-2\mu \tilde{\mathcal{C}}_G(x)}$. Thus the expression in the first set of parentheses can be replaced by $\sqrt{(2/\mu)} \tilde{\pi}(x)$ and the whole integral reduces to

$$a(t) \int_\Sigma d^3x [\tilde{\pi}(x) - \sqrt{-2\mu \tilde{\mathcal{C}}_G(x)}] \equiv 0. \quad (7)$$

Note that we assume that the Hamiltonian constraint $\mathcal{C}_G(x)$ satisfies the weak energy condition [13], which in this case requires that $\mathcal{C}_G(x) \leq 0$.

In the process of quantization we promote this constraint into an operator equation. We require that in the loop representation the spin network states, depending also on the clock variable T , be annihilated by the constraint operator:

$$\langle S, T | a(t) \int_\Sigma d^3x \left[\hat{\tilde{\pi}}(x) - \sqrt{-2\mu \hat{\mathcal{C}}_G(x)} \right] = 0. \quad (8)$$

We interpret the integral

$$\int_\Sigma d^3x \hat{\tilde{\pi}}(x)$$

as $i\hbar$ times a derivative with respect to the ‘‘clock’’ field and thus we arrive at the Schrödinger equation

$$i\hbar \frac{\partial}{\partial T} \langle S, T | = \langle S, T | \hat{H}, \quad (9)$$

where the Hamiltonian \hat{H} corresponds to the classical observable² (we have restored the constants)

$$H = \frac{\sqrt{\mu}}{\sqrt{4\pi G}} \int_\Sigma d^3x \sqrt{-C(x) + \Lambda q(x)}, \quad (10)$$

where

²The same result can be obtained [7] by imposing gauge fixing at the Lagrangian level and after that performing the Legendre transformation.

$$-C(x) + \Lambda q(x) = -\epsilon_{ijk} \left\{ F_{ab}^k \tilde{E}^{ai} \tilde{E}^{bj} - \frac{1}{3!} \Lambda \epsilon_{abc} \tilde{E}^{ai} \tilde{E}^{bj} \tilde{E}^{ck} \right\}. \quad (11)$$

We will omit the overall factor of $(\sqrt{\mu}/\sqrt{4\pi G})$ in what follows, as it is not important for our considerations.

Because of the product of distributional quantities in the Hamiltonian, we have to regulate the above expression. Using an arbitrary, e.g., Euclidian, background metric $h_{ab}(x)$, we divide the space manifold Σ into cubes of size L , labeled R_I . In the calculations we will let L to go to zero as the number of cubes goes to infinity. Then we can write Eq. (10) as

$$H = \lim_{L \rightarrow 0} \sum_I \int_{R_I} d^3x \sqrt{h(x)} \sqrt{\frac{-C(x) + \Lambda q(x)}{h(x)}} \\ = \lim_{L \rightarrow 0} \sum_I L^3 \sqrt{\frac{-C(x_I) + \Lambda q(x_I)}{h(x_I)}}, \quad (12)$$

where $h(x)$ is the determinant of the background metric and x_I in the last expression is a point in the cube R_I . Now putting L^3 inside the square root and going back to integral form, we get

$$H = \lim_{L \rightarrow 0} \sum_I \sqrt{L^3 \int_{R_I} \frac{d^3x}{\sqrt{h(x)}} [-C(x) + \Lambda q(x)]} \\ = \lim_{L \rightarrow 0} \sum_I \sqrt{-C_I + \Lambda V_I^2}. \quad (13)$$

All of the above manipulations are correct in the limit $L \rightarrow 0$. The last step in Eq. (13) is a definition of C_I . V_I is the classical volume of the I th cube.

Let us now focus on the first term of the expression under the square root in Eq. (13). We introduce a regulating point-splitting function $f_\delta(\tilde{x}, y)$, which is a density of weight 1 with respect to its first argument. This function satisfies the requirement that for any smooth function $\phi(x)$:

$$\lim_{\delta \rightarrow 0} \int_{R_I \ni y} d^3x \phi(x) f_\delta(\tilde{x}, y) = \phi(y). \quad (14)$$

Using the regulating function we can write C_I as

$$C_I = \lim_{\delta \rightarrow 0} \epsilon_{ijk} L^3 \int_{R_I} \frac{d^3x}{\sqrt{h(x)}} F_{ab}^k(x) \int_{R_I} d^3y f_\delta(\tilde{x}, y) \tilde{E}^{ai}(y) \\ \times \int_{R_I} d^3z f_\delta(\tilde{x}, z) \tilde{E}^{bj}(z). \quad (15)$$

To ensure proper contractions of the internal indices in the last expression, we connect the points x , y , and z with holonomies of the Ashtekar connection along some smooth paths γ_1 and γ_2 connecting the points. We also use the identity $\epsilon_{ijk} = -4 \text{Tr}[\tau_i \tau_j \tau_k]$ to write Eq. (15) as

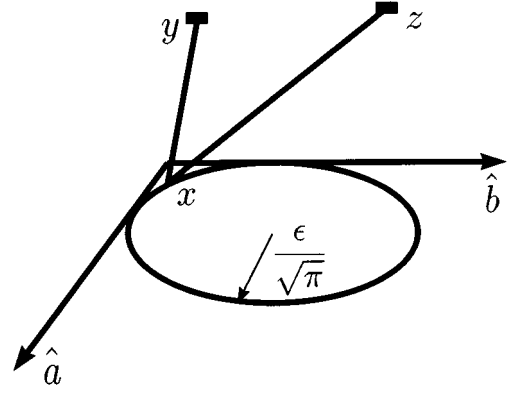


FIG. 1. Loop $\gamma_{x, [\hat{a}\hat{b}]}^{\epsilon^2} \# \gamma_{xyx} \# \gamma_{xzx}$ on which the T operator is based.

$$C_I = -\lim_{\delta \rightarrow 0} 4L^3 \int_{R_I} \frac{d^3x}{\sqrt{h(x)}} \int_{R_I} d^3y f_\delta(\tilde{x}, y) \\ \times \int_{R_I} d^3z f_\delta(\tilde{x}, z) \text{Tr}[F_{ab}^k(x) \tau_k U_{\gamma_1}(x, y) \tilde{E}^{ai}(y) \tau_i \\ \times U_{\gamma_1^{-1}}(y, x) U_{\gamma_2}(x, z) \tilde{E}^{bj}(z) \tau_j U_{\gamma_2^{-1}}(z, x)]. \quad (16)$$

To complete the regularization, we also replace the curvature $F_{ab}^k(x)$ by its approximation by a holonomy:

$$F_{ab}^k(x) \tau_k = \lim_{\epsilon \rightarrow 0} \frac{1}{2\epsilon^2} U(\gamma_{x, [\hat{a}\hat{b}]}^{\epsilon^2}),$$

where $\gamma_{x, [\hat{a}\hat{b}]}^{\epsilon^2}$ is a loop with area ϵ^2 in the (\hat{a}, \hat{b}) coordinate plane, based at the point x . We have included explicitly the antisymmetrization with respect to \hat{a} and \hat{b} to ensure the vanishing of first term in the expansion of the holonomy $U(\gamma_{x, [\hat{a}\hat{b}]}^{\epsilon^2})$ in powers of ϵ^2 . Thus for C_I we get

$$C_I = -\lim_{\epsilon \rightarrow 0} \lim_{\delta \rightarrow 0} \frac{L^3}{2\epsilon^2} \int_{R_I} \frac{d^3x}{\sqrt{h(x)}} \int_{R_I} d^3y f_\delta(\tilde{x}, y) \\ \times \int_{R_I} d^3z f_\delta(\tilde{x}, z) \text{Tr}[U(\gamma_{x, [\hat{a}\hat{b}]}^{\epsilon^2}) U_{\gamma_1}(x, y) \tilde{E}^a(y) \\ \times U_{\gamma_1^{-1}}(y, x) U_{\gamma_2}(x, z) \tilde{E}^b(z) U_{\gamma_2^{-1}}(z, x)],$$

where we have used the convention $2\tilde{E}^{ai}(y) \tau_i = \tilde{E}^a(y)$. The expression under the trace is exactly a Smolin-Rovelli [4] loop variable $-T^{[ab]}(\gamma_{x, [\hat{a}\hat{b}]}^{\epsilon^2} \# \gamma_{xyx} \# \gamma_{xzx})$ based on the loop shown in Fig. 1. Thus finally we get, for the regulated version of C_I ,

$$C_I = \lim_{\epsilon \rightarrow 0} \lim_{\delta \rightarrow 0} C_I^{L, \delta, \epsilon},$$

where

$$C_I^{L, \delta, \epsilon} = \frac{L^3}{2\epsilon^2} \int_{R_I} \frac{d^3x}{\sqrt{h(x)}} \int_{R_I} d^3y f_\delta(\tilde{x}, y) \int_{R_I} d^3z f_\delta(\tilde{x}, z) \times \sum_{\hat{ab}} T^{[ab]}(\gamma_{x, \hat{ab}}^{\epsilon^2} \# \gamma_{xyx} \# \gamma_{zxx}). \tag{17}$$

Now we promote the last expression into an operator by replacing the loop variable $T^{[ab]}$ with the corresponding loop operator. Thus for the Hamiltonian operator \hat{H} we get

$$\hat{H} = \lim_{L \rightarrow 0} \sum_I^\infty \sqrt{-\lim_{\epsilon \rightarrow 0} \lim_{\delta \rightarrow 0} \hat{C}_I^{L, \delta, \epsilon} + \Lambda \hat{V}_I^2}, \tag{18}$$

where \hat{V}_I is the volume operator, as defined in [12]. As was shown in [12], the spin network states are eigenstates of the volume operator, and so we can replace \hat{V}_I with the corresponding eigenvalue for the volume of the I th cube.

Thus we have a regulated version of the Hamiltonian operator with which we act on the spin network states. We follow the standard procedure of regularization in which we apply the Hamiltonian on the states, perform all integrations, and at the end take the limits.

Definitions of the spin network states can be found in [8–10, 12]. For our purposes it suffices to recall just the basic components of the definition. The spin networks are defined by a closed graph Γ in three-space, labeling of the edges by irreducible representations of $SU(2)$ (we can interpret the labels as giving the number of loop segments along the corresponding edge), and intertwiners at the vertices, defining the way the loop segments coming from the edges are routed through the vertex.

For a rigorous description of the way the spin networks are projected on a plane, we would need some additional details, but for simplicity in our calculations we will assume that the spin network we are using has been already projected.

In our work we introduce a modification of the definition of the loop operators. In their standard definition, the loop operators $\hat{T}^{ab}[\gamma]$ are based on a loop γ and corresponding to every index there is a ‘‘hand’’ attached to the loop γ . In our case, because the loop on which \hat{T}^{ab} is based shrinks to a point, we have the freedom of modifying the attachment of the ‘‘hands’’ in a way convenient for our calculations. We consider the base loop γ to be a planar loop with ‘‘hands’’ based on spin network edges of infinitesimal length δ attached to γ . These edges have color 2 and are denoted γ_{xyx} and γ_{zxx} in Eq. (17). It will be also convenient for us to split the points at which the ‘‘hands’’ are attached to the loop γ so that there is a distance of order δ between them. This can be thought of as a choice of decomposition of the four-valent vertex positioned at the point x into two trivalent vertices.

With such a definition it can be easily shown that the standard action of the ‘‘hands’’ is represented by connecting

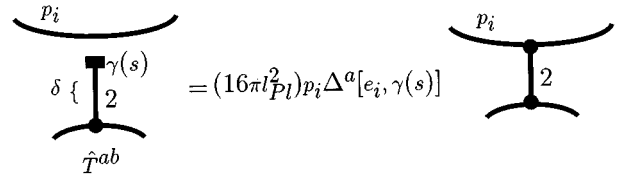


FIG. 2. Action of a ‘‘hand’’ of the \hat{T}^{ab} operator.

the spin network, on which \hat{T}^{ab} is based, by edges of color 2 to the original spin network. At the place of each grasping, the action creates new trivalent vertices. Also, we multiply by a factor of $16\pi l_P^2 p_i \Delta^a[e_i, \gamma(s)]$ whenever a ‘‘hand’’ situated at $\gamma(s)$, corresponding to a index ‘‘a’’ of the loop operator, grasps an edge, e_i of color p_i from the spin network l_P is the Planck length, and $\Delta^a[e_i, \gamma(s)]$ is the standard distributional expression:

$$\Delta^a[e_i, \gamma(s)] = \oint dt \dot{e}_i(t) \delta^3(\gamma(s), e_i(t)).$$

The action of one of the ‘‘hands’’ of the \hat{T}^{ab} operator is shown in Fig. 2. Now we are in position to apply the Hamiltonian operator to the spin network states. We also assume that the spin network states are normalized as in [12]. For the action of the Hamiltonian on $\langle S, T |$, we get

$$\begin{aligned} \langle S, T | \hat{C}_I^{L, \delta, \epsilon} &= \frac{L^3}{2\epsilon^2} \int_{R_I} \frac{d^3x}{\sqrt{h(x)}} \int_{R_I} d^3y f_\delta(\tilde{x}, y) \int_{R_I} d^3z f_\delta(\tilde{x}, z) \\ &\times \sum_{\hat{ab}} \left\{ \sum_i \langle e_i | \hat{T}^{[ab]}(\gamma_{x, \hat{ab}}^{\epsilon^2} \# \gamma_{xyx} \# \gamma_{zxx}) \right. \\ &\left. + \sum_k \sum_{i,j} \langle e_i^{(k)}, e_j^{(k)} | \hat{T}^{[ab]}(\gamma_{x, \hat{ab}}^{\epsilon^2} \# \gamma_{xyx} \# \gamma_{zxx}) \right\}. \end{aligned} \tag{19}$$

In the first term of the above, the sum i runs over all edges in the I th cube. In the second term, the index k runs over all vertices inside the I th cube and the indices i and j run over all edges joined at the k th vertex. We get two types of terms: edge terms and vertex terms. In an edge term, the two ‘‘hands’’ of the Hamiltonian grasp one and the same edge of the spin network, labeled e_i , having color p_i . In vertex terms the two ‘‘hands’’ grasp two different edges $e_i^{(k)}$ and $e_j^{(k)}$, joined at a vertex v_k . The two edges in general have different colors p_i and p_j . We divide the vertex terms further into two subcases: Either the tangents to the edges at the common vertex are collinear, or there is some angle θ , different from 0° and 180° , between the tangents.

We will assume that the cubes have been shrunk enough so that in a single cube there is at most one vertex. The

evaluation of the action in any case can be split into two different parts—we have an analytical part, coming from calculating the prefactors in the action of the “hands” and evaluating the integrals, and a graphical part in which we complete the limiting procedure by shrinking the attached loops.

III. ANALYTICAL ACTION OF THE HAMILTONIAN OPERATOR ON SPIN NETWORK STATES

A. Action on a single edge

For the first type of terms in the last set of brackets in Eq. (19), we get

$$\begin{aligned} & \frac{L^3}{2\epsilon^2} \int_{R_I} \frac{d^3x}{\sqrt{h(x)}} \int_{R_I} d^3y f_\delta(\vec{x}, y) \int_{R_I} d^3z f_\delta(\vec{x}, z) \sum_{\hat{a}\hat{b}} \langle e_i | \hat{T}^{[ab]} (\gamma_{x,\hat{a}\hat{b}}^{\epsilon^2} \# \gamma_{xyx} \# \gamma_{xzx}) \\ & = \frac{L^3}{2\epsilon^2} (16\pi l_{\text{pl}}^2)^2 p_i^2 \int_I ds \int_I dt \int_{R_I} \frac{d^3x}{\sqrt{h(x)}} f_\delta(\vec{x}, e_i(s)) f_\delta(\vec{x}, e_i(t)) \sum_{\hat{a}\hat{b}} \dot{e}_i^{[a]}(s) \dot{e}_i^{[b]}(t) \langle e_i \# \gamma_{x,\hat{a}\hat{b}}^{\epsilon^2} \# \gamma_{xyx} \# \gamma_{xzx} |. \end{aligned} \quad (20)$$

The meaning of the notation in $\langle e_i \# \gamma_{x,\hat{a}\hat{b}}^{\epsilon^2} \# \gamma_{xyx} \# \gamma_{xzx} |$ can be understood from Fig. 3. The dashed circle denotes the region which will be shrunk to a point. To proceed further we have to specify the regulating function $f_\delta(\vec{x}, y)$. We use a normalized, weighted θ function:

$$f_\delta(\vec{x}, y) = \sqrt{h(x)} f_\delta(x, y) = \left(\frac{3}{4\pi\delta^3} \right) \sqrt{h(x)} \theta[\delta - |\vec{x} - \vec{y}|]. \quad (21)$$

After evaluation of the space integral in Eq. (20), we get

$$\begin{aligned} & \int_{R_I} \frac{d^3x}{\sqrt{h(x)}} f_\delta(\vec{x}, e_i(s)) f_\delta(\vec{x}, e_i(t)) \\ & = \frac{3}{8\pi\delta^3} \left[2 - \frac{3}{2} \frac{d}{\delta} + \left(\frac{d}{2\delta} \right)^3 \right], \end{aligned} \quad (22)$$

for $d = d(s, t) = |\vec{e}_i(s) - \vec{e}_i(t)|$ less than 2δ and zero otherwise. We have assumed also that $\delta < L$.

As we are going to let δ to go to zero, this will force also the separation between $\vec{e}_i(s)$ and $\vec{e}_i(t)$ to approach zero. This is why we keep one of the parameters, say, s , fixed and expand $\vec{e}_i(t)$ in power series about s . The first term in the

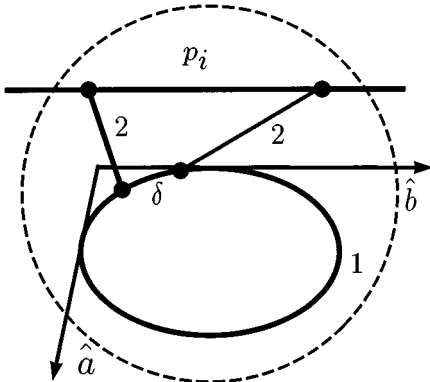


FIG. 3. Grasping of the Hamiltonian on a single edge.

expansion will make the whole expression vanishing, because of the antisymmetrization of the product $\dot{e}_i^{[a]}(s) \dot{e}_i^{[b]}(s)$. Also, the distance d can be replaced by $|(t-s)| |\dot{e}_i(s)|$. Combining Eqs. (20) and (22), we get, to the lowest order in δ ,

$$\begin{aligned} & \frac{L^3}{\epsilon^2 \delta^3} \frac{3}{16\pi} (16\pi l_{\text{pl}}^2)^2 p_i^2 \int_I ds \int_I dt \\ & \times \left[2 - 3 \frac{|(t-s)| |\dot{e}_i(s)|}{2\delta} + \left(\frac{|(t-s)| |\dot{e}_i(s)|}{2\delta} \right)^3 \right] \\ & \times \sum_{\hat{a}\hat{b}} |t-s| \dot{e}_i^{[a]}(s) \dot{e}_i^{[b]}(s) \langle e_i \# \gamma_{x,\hat{a}\hat{b}}^{\epsilon^2} \# \gamma_{xyx} \# \gamma_{xzx} |. \end{aligned} \quad (23)$$

The limits of integration with respect to t are determined again by the expansion of $d(s, t)$ and are given by

$$t \in \left[s - \frac{2\delta\delta^-}{|\dot{e}_i(s)|}, s + \frac{2\delta\delta^+}{|\dot{e}_i(s)|} \right],$$

where $\delta^+ = 1 + O(\delta)$ and $\delta^- = 1 - O(\delta)$. As the integrals with respect to s and t are reparametrization invariant, we can choose a parametrization such that $|\dot{e}_i(s)| = 1$. In this parametrization we set

$$\vec{e}_i(s) \equiv \hat{\tau}$$

and

$$\vec{e}_i(s) = \frac{\hat{n}}{\rho(s)},$$

where $\hat{\tau}$ and \hat{n} are the unit tangent and normal vectors to the loop and $\rho(s)$ is the curvature radius of the loop. Now we can perform the integration with respect to t and get

$$\int_{s-2\delta\delta^-}^{s+2\delta\delta^+} dt |t-s| \left[2 - 3 \frac{|(t-s)|}{2\delta} + \left(\frac{|(t-s)|}{2\delta} \right)^3 \right]$$

$$= 8\delta^2 \left(\frac{1}{5} + O(\delta) \right).$$

Thus for Eq. (23) we obtain

$$\frac{L^3}{\epsilon^2 \delta} \frac{3}{10\pi} (16\pi l_{\text{Pl}}^2)^2 p_i^2 \int_I \frac{ds}{\rho(s)} \sum_{\hat{a}\hat{b}} \hat{\tau}^{[a}(s) \hat{n}^{b]}(s)$$

$$\times \langle e_i \# \gamma_{x,\hat{a}\hat{b}}^{\epsilon^2} \# \gamma_{xyx} \# \gamma_{xzx} \rangle.$$

Using the corresponding expression from connection representation in terms of holonomies, it can be shown that up to terms of order ϵ the last sum can be written as

$$\sum_{\hat{a}\hat{b}} \hat{\tau}^{[a}(s) \hat{n}^{b]}(s) \langle e_i \# \gamma_{x,\hat{a}\hat{b}}^{\epsilon^2} \# \gamma_{xyx} \# \gamma_{xzx} \rangle$$

$$= \langle e_i \# \gamma_{x,\hat{\tau}\hat{n}}^{\epsilon^2} \# \gamma_{xyx} \# \gamma_{xzx} \rangle, \quad (24)$$

where now the loop $\gamma_{x,\hat{\tau}\hat{n}}^{\epsilon^2} \# \gamma_{xyx} \# \gamma_{xzx}$ is in a plane defined by the tangent and the normal to the edge e_i at the point s . Note that this loop is well defined as in the terms where the edge is a straight line and the normal is not defined the curvature radius becomes infinite and such terms vanish. In the general case since the size L of the cubes goes to zero, we can replace the integral with respect to s by its mean value:

$$\int_I \frac{ds}{\rho(s)} \langle e_i \# \gamma_{x,\hat{\tau}\hat{n}}^{\epsilon^2} \# \gamma_{xyx} \# \gamma_{xzx} \rangle$$

$$= \frac{\kappa L}{\rho_I} \langle e_i \# \gamma_{x,\hat{\tau}\hat{n}}^{\epsilon^2} \# \gamma_{xyx} \# \gamma_{xzx} \rangle_I,$$

where κ is a number of order 1, depending on the orientation of the edge inside the cube. We finally get the analytical expression for the action of the Hamiltonian on a single smooth edge:

$$\frac{\kappa L^4}{\epsilon^2 \rho_I \delta} \frac{3}{10\pi} (16\pi l_{\text{Pl}}^2)^2 p_i^2 \langle e_i \# \gamma_{x,\hat{\tau}\hat{n}}^{\epsilon^2} \# \gamma_{xyx} \# \gamma_{xzx} \rangle_I. \quad (25)$$

This expression is a product of a prefactor, containing a combination of regulating parameters and the original spin network with attached additional loops, subject to graphical evaluation. The prefactor will determine the way in which we take the three limits $\epsilon \rightarrow 0$, $\delta \rightarrow 0$, and $L \rightarrow 0$ to make the whole expression finite.

To understand the above intermediate result, we compute the action of the regulated diffeomorphism constraint:

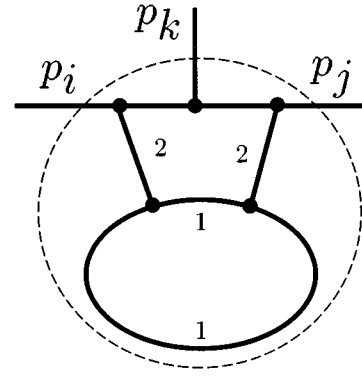


FIG. 4. Grasping of the Hamiltonian on two edges meeting at a vertex and having collinear tangents.

$$\hat{C}(\vec{N}) = \lim_{L \rightarrow 0} \sum_I \lim_{\delta \rightarrow 0} \lim_{\epsilon \rightarrow 0} \frac{1}{\epsilon^2} \sum_{ab} \int_{R_I} d^3x N^a(x)$$

$$\times \int_{R_I} d^3y f_\delta(\vec{x}, y) \hat{T}^b[\gamma_{x,ab}^{\epsilon^2} \# \gamma_{xyx}], \quad (26)$$

on a single smooth edge of the spin network state. The result, up to finite numerical factors, is the same as Eq. (25) if the shift vector $N^a(x)$ is given by

$$N^a(s) = \hat{n}^a(s) \frac{L^3}{\rho(s) \delta}. \quad (27)$$

This is not surprising since a similar result is true for the calculation in the connection representation. To obtain this result, one also must perform the graphical evaluation of the loop $\gamma_{x,\hat{\tau}\hat{n}}^{\epsilon^2} \# \gamma_{xyx} \# \gamma_{xzx}$ from Eq. (25) and of the loop $\gamma_{x,\hat{\tau}\hat{n}}^{\epsilon^2} \# \gamma_{xyx}$ from the calculation of the action of the diffeomorphism constraint, which shrink at the end of the calculations. We show in detail this evaluation later in the paper in Sec. IV A.

Thus the action of the Hamiltonian on smooth edges of the spin network states can be interpreted as diffeomorphism transformation in a direction defined by Eq. (27). This means that if we act on diffeomorphism-invariant states, the action of the Hamiltonian on edges annihilates them. As we assume that the states we act on a diffeomorphism invariant, we will discard the action on smooth edges from the final result.

B. Action on two edges meeting at a vertex with collinear tangents

An example of the grasping of the Hamiltonian on two edges meeting at a vertex and having collinear tangents is shown in Fig. 4. The analytical calculation in this case is almost the same as with the case of a single edge. The only difference comes from the fact that the grasped edges could have different colors, and so instead of Eq. (25) we have

$$\frac{\kappa L^4}{\epsilon^2 \rho_I \delta} \frac{3}{10\pi} (16\pi l_{\text{Pl}}^2)^2 p_i p_j \langle (e_i, e_j) \# \gamma_{x, \hat{\eta}}^{\epsilon^2} \# \gamma_{xyx} \# \gamma_{xzx} |_I \rangle. \quad (28)$$

In this case we cannot interpret the action of the Hamiltonian as a diffeomorphism transformation. As discussed in [14], in such cases the action can change the diffeomorphism class of the spin network. But as we will see later in the paper, such terms are of order L and they vanish after taking all limits.

C. Action on two edges meeting at a vertex with noncollinear tangents

Let the Hamiltonian grasp the edges e_i and e_j with colors p_i and p_j , respectively. Let e_i and e_j meet at some vertex u_k . We denote the part of the spin network state corresponding to the edges under consideration by $\langle (e_i, e_j) |$. For the action of the Hamiltonian we have

$$\begin{aligned} \langle (e_i, e_j) | & \frac{L^3}{2\epsilon^2} \int_{R_I} \frac{d^3x}{\sqrt{h(x)}} \int_{R_I} d^3y f_\delta(\tilde{x}, y) \int_{R_I} d^3z f_\delta(\tilde{x}, z) \hat{T}^{[ab]} (\gamma_{x, \hat{a}\hat{b}}^{\epsilon^2} \# \gamma_{xyx} \# \gamma_{xzx}) \\ & = \frac{L^3}{2\epsilon^2} (16\pi l_{\text{Pl}}^2)^2 p_i p_j \int_I ds \int_I dt \int_{R_I} \frac{d^3x}{\sqrt{h(x)}} f_\delta(\tilde{x}, e_i(s)) f_\delta(\tilde{x}, e_j(t)) \sum_{\hat{a}\hat{b}} \dot{e}_i^{[a]}(s) \dot{e}_j^{b]}(t) \langle (e_i, e_j) \# \gamma_{x, \hat{a}\hat{b}}^{\epsilon^2} \# \gamma_{xyx} \# \gamma_{xzx} |. \end{aligned} \quad (29)$$

Again $\langle (e_i, e_j) \# \gamma_{x, \hat{a}\hat{b}}^{\epsilon^2} \# \gamma_{xyx} \# \gamma_{xzx} |$ denotes the action of grasping of the Hamiltonian. Using Eq. (22), we can evaluate the spatial integral to get

$$\frac{L^3}{\epsilon^2 \delta^3} \frac{3}{16\pi} (16\pi l_{\text{Pl}}^2)^2 p_i p_j \int_I ds \int_I dt \left[2 - 3 \frac{|\vec{e}_i(s) - \vec{e}_j(t)|}{2\delta} + \left(\frac{|\vec{e}_i(s) - \vec{e}_j(t)|}{2\delta} \right)^3 \right] \sum_{\hat{a}\hat{b}} \dot{e}_i^{[a]}(s) \dot{e}_j^{b]}(t) \langle (e_i, e_j) \# \gamma_{x, \hat{a}\hat{b}}^{\epsilon^2} \# \gamma_{xyx} \# \gamma_{xzx} |. \quad (30)$$

We use a parametrization such that $|\dot{e}_i| = |\dot{e}_j| = 1$, and so the distance $d(s, t) = |\vec{e}_i(s) - \vec{e}_j(t)|$ becomes simply $d(s, t) = |s - t|$. Also, let η and ζ be the unit tangent vectors at the vertex, and let the angle between them be θ_{ij} . Performing the integration with respect to s and t we get, for Eq. (30),

$$\frac{L^3}{\epsilon^2 \delta} \frac{3\theta_{ij}}{10\pi \sin\theta} (16\pi l_{\text{Pl}}^2)^2 p_i p_j \sum_{\hat{a}\hat{b}} \hat{\eta}^{[a} \hat{\zeta}^{b]} \langle (e_i, e_j) \# \gamma_{x, \hat{a}\hat{b}}^{\epsilon^2} \# \gamma_{xyx} \# \gamma_{xzx} |.$$

Again, we can use a formula which can be proved by using the corresponding expression in the connection representation: namely,

$$\sum_{\hat{a}\hat{b}} \hat{\eta}^{[a} \hat{\zeta}^{b]} \langle (e_i, e_j) \# \gamma_{x, \hat{a}\hat{b}}^{\epsilon^2} \# \gamma_{xyx} \# \gamma_{xzx} | = \sin\theta \langle (e_i, e_j) \# \gamma_{x, \hat{\eta}\hat{\zeta}}^{\epsilon^2} \# \gamma_{xyx} \# \gamma_{xzx} |,$$

to transform the sum in Eq. (30). In the last expression, $\gamma_{x, \hat{\eta}\hat{\zeta}}^{\epsilon^2}$ is a loop in the plane defined by the two tangent vectors $\hat{\eta}$ and $\hat{\zeta}$. Thus finally we get for the action of the Hamiltonian on a vertex:

$$\frac{L^3}{\epsilon^2 \delta} \frac{3\theta_{ij}}{10\pi} (16\pi l_{\text{Pl}}^2)^2 p_i p_j \langle (e_i, e_j) \# \gamma_{x, \hat{\eta}\hat{\zeta}}^{\epsilon^2} \# \gamma_{xyx} \# \gamma_{xzx} |. \quad (31)$$

In the obtained expression, we can separate between the prefactor and loop-deformed spin network state. The prefactor contains a combination of the regulating parameters and an implicit dependence on the arbitrary background metric through the angle θ_{ij} . The loop deformation will be subject to a graphical evaluation later in the paper.

D. Taking the limits

Now we are in position to take the limits in the computation. Basically, the limits appear in our calculation in two

different ways. First, the prefactors in Eqs. (28) and (31) contain combinations of the regulating parameters. The limits should be taken in such a way so that these combinations yield finite results. Second, the loop on which the loop operator \hat{T}^{ab} is based shrinks to a point, together with its ‘‘hands,’’ and this leads to the graphical evaluation.

The combinations of parameters are

$$\frac{\kappa L^4}{\epsilon^2 \delta} \quad \text{and} \quad \frac{L^3}{\epsilon^2 \delta} \quad (32)$$

for Eqs. (28) and (31), respectively. To ensure finiteness of our expressions, let us take the three limits $\epsilon \rightarrow 0$, $\delta \rightarrow 0$, and $L \rightarrow 0$ along a plane in the (L, ϵ, δ) parameter space, defined by

$$\frac{L^3}{\epsilon^2 \delta} = Z,$$

where Z is an arbitrary constant, chosen in such a way so the relative order of taking the limits is satisfied. This order is determined by the conditions that $\delta < L$ and $\delta \ll \epsilon$. We have to be careful about the way the limits in L and δ are taken, as the diffeomorphism vector (27) contains the ratio L^3/δ , and so we would not like δ to go to zero much faster than L . If we set $L^3/\delta = \text{const}$, then this will be enough to prevent the diffeomorphism from becoming infinite.

We can now write the general formula for the analytical action of the Hamiltonian on diffeomorphism-invariant spin network states. All the cubes which are empty give zero.

The result from the action on different edges meeting at a vertex with collinear tangents (28) can be written as

$$\frac{3\kappa ZL}{10\pi\rho_l} (16\pi l_{\text{Pl}}^2)^2 p_i p_j \langle (e_i, e_j) \# \gamma_{x, \hat{m}}^{\epsilon^2} \# \gamma_{xyx} \# \gamma_{xzx} |$$

and vanishes as L goes to zero.

Adding up all contributions from the vertices with non-collinear tangents, we get

$$\langle S, T | \hat{C}_l^{L, \delta, \epsilon} = \frac{3Z}{10\pi} (16\pi l_{\text{Pl}}^2)^2 \sum_{i,j} p_i p_j \theta_{ij} \overline{\langle (e_i^{(k)}, e_j^{(k)}) \# \gamma_{x, \hat{\eta}_k}^{\epsilon^2} \# \gamma_{xyx} \# \gamma_{xzx} |}. \quad (33)$$

In the above sums, the indices i and j run over all edges joined at the vertex v_k which is in the l th cube. The sum contains the arbitrary but finite constant Z and the angle θ_{ij} between the edges at the vertex v_k . The bar over the state represents the fact that we still have to perform the shrinking of the attached loops and thus to evaluate the graph.

We get an overall action which is finite but background dependent because of the presence of the angle θ_{ij} . This is a problem which can be solved by redefining the way we approximate the curvature F_{ab} . Let the holonomy which approximates the curvature be based on a loop with area $\theta_{ij}\epsilon^2$ instead of ϵ^2 . Then all the calculations go through, but at the end there is an extra factor of θ_{ij} in the denominator of Eq. (33) to cancel the corresponding factor from the numerator. It is important to notice that although the explicit inclusion of the factor of θ_{ij} formally solves the problem of background dependence, the situation is not completely satisfactory. The computation of the evolution of the spin network states involves at each step measuring the angle θ_{ij} between each pair of tangent vectors. Technically, this might require the introduction in the definition of the Hamiltonian of an operator, measuring the angle θ_{ij} . This issue requires further investigation.

IV. GRAPHICAL ACTION OF THE HAMILTONIAN

To evaluate the deformed spin network state from Eq. (33), we use some techniques from the recoupling theory of colored trivalent links and knots. First, let us consider a general situation in which a loop attached to a spin network is shrunk to a point. An important observation is that the evaluation is local, in the sense that whatever result we obtain, it is independent of the way the spin network is connected outside of the circle denoting the shrinking region.

To evaluate the attached loop we have to do the following: Expand all the edges which are entirely in the shrinking region as an antisymmetrized sum with all possible crossings between the loop segments; resolve each crossing of single loop segments in the shrinking region according to the binor Mandelstam identity (see [12] for a discussion); associate to each closed single loop the ‘‘loop value’’ (-2) ; smooth the obtained graph to get if possible the original spin network.

But these are exactly the operations which occur in the evaluation of the Kauffman bracket [15]. The Kauffman bracket is an invariant of the regular isotopy of colored knots and links with trivalent vertices. Thus, for the evaluation of the graphical action of the loop operators, we can use the techniques of recoupling theory, developed for computing the Kauffman bracket [15,16,18,12]. What makes these techniques powerful is the fact that we do the computations blockwise. First, we work out the analytical expressions for the most simple graphs. Then in more complicated calculations we identify the simple graphs and replace them with the corresponding analytical expressions. This is possible because the evaluation of the graphs is local—we can shrink to a point just a portion of the whole graph, keeping the remaining parts fixed. The basic formulas of the recoupling theory are summarized in the Appendix. With the use of these formulas, we compute the graphical action of the Hamiltonian on smooth edges and on vertices.

A. Evaluation of the graphical action for edges

We perform the graphical evaluation for the grasp of a smooth edge to show that the graphical action of the Hamiltonian on smooth edges is equivalent to a diffeomorphism transformation. We start from the expression $\langle e_i \# \gamma_{x, \hat{m}}^{\epsilon^2} \# \gamma_{xyx} \# \gamma_{xzx} |$. The grasping is shown in Fig. 3. First, we use the basic recoupling formula (A1) from the Appendix on one of the edges. As a result, a new link of color n appears in the new configuration. The allowed values for n are determined by the basic properties of the trivalent vertices—the only values it can take are $p_i \pm 1$:

$$\langle e_i \# \gamma_{x, \hat{m}}^{\epsilon^2} \# \gamma_{xyx} \# \gamma_{xzx} | = \sum_{n=p_i \pm 1} \left\{ \begin{matrix} p_i & p_i & n \\ 1 & 1 & 2 \end{matrix} \right\} \langle \text{graph with loop of color } n \rangle$$

On the right-hand side appears the $6j$ symbol, as defined in [15]. We repeat the same step with the other ‘‘hand’’ and get

$$\sum_{n=p_i \pm 1} \sum_{m=p_i \pm 1} \left\{ \begin{matrix} p_i & p_i & n \\ 1 & 1 & 2 \end{matrix} \right\} \left\{ \begin{matrix} p_i & p_i & m \\ 1 & 1 & 2 \end{matrix} \right\} \text{Diagram}$$

As a next step, we remove the internal ‘bubble’ using the ϑ net from Eq. (A4) from the Appendix to obtain

$$\langle e_i \# \gamma_{x, \hat{\tau} \hat{n}}^{\epsilon^2} \# \gamma_{xyx} \# \gamma_{zxx} | = \sum_{n=p_i \pm 1} (-1)^n \left\{ \begin{matrix} p_i & p_i & n \\ 1 & 1 & 2 \end{matrix} \right\}^2 \frac{\vartheta(p_i, 1, n)}{n+1} \text{Diagram}$$

To continue further we have to make a more careful analysis of the way the limit is taken, when the states are diffeomorphism invariant. As this is not relevant for our considerations, we will stop here and show that the above expression is analogous to the result from the action of the diffeomorphism constraint. To this aim we act with Eq. (26) on a smooth edge. There, the loop deformation is given by the expression $\gamma_{x, \hat{\tau} \hat{n}}^{\epsilon^2} \# \gamma_{xyx}$. To evaluate graphically this expression, we use the basic recoupling formula (A1) and immediately get

$$\langle e_i \# \gamma_{x, \hat{\tau} \hat{n}}^{\epsilon^2} \# \gamma_{xyx} | = \text{Diagram} = \sum_{n=p_i \pm 1} \left\{ \begin{matrix} p_i & p_i & n \\ 1 & 1 & 2 \end{matrix} \right\} \text{Diagram}$$

Thus we see that in both cases of the action of the Hamiltonian and of the diffeomorphism constraints, the graphical evaluation leads to the a ‘bubble’ on the smooth edge with different numerical factors. This proves that the two graphical actions are equivalent, and thus we can disregard all terms in the action of the Hamiltonian on smooth edges of diffeomorphism-invariant states.

B. Evaluation of the graphical action for vertices

We apply the techniques from the recoupling theory of colored graphs also to evaluate the action of the Hamiltonian when it grasps two edges meeting at a vertex. For simplicity, we consider only the action on one pair of edges joint at a trivalent vertex. We have initially the expression $\langle (e_i, e_j) \# \gamma_{x, \hat{\eta} \hat{\zeta}}^{\epsilon^2} \# \gamma_{xyx} \# \gamma_{zxx} |$, which can be transformed with the use of the recoupling formula (A1), given in the Appendix. We obtain the result

$$\langle (e_i, e_j) \# \gamma_{x, \hat{\eta} \hat{\zeta}}^{\epsilon^2} \# \gamma_{xyx} \# \gamma_{zxx} | = \text{Diagram} = \sum_{n=p_i \pm 1} \left\{ \begin{matrix} p_i & p_i & n \\ 1 & 1 & 2 \end{matrix} \right\} \text{Diagram}$$

Then we repeat the same step with the other ‘hand’ of the T operator to get

$$\sum_{n=p_i \pm 1} \sum_{m=p_j \pm 1} \left\{ \begin{matrix} p_i & p_i & n \\ 1 & 1 & 2 \end{matrix} \right\} \left\{ \begin{matrix} p_j & p_j & m \\ 1 & 1 & 2 \end{matrix} \right\} \text{Diagram}$$

The inner triangular diagram of the above graph can be evaluated with the use of one recoupling formula and one ‘bubble’ removal (see the Appendix):

$$\langle (e_i, e_j) \# \gamma_{x, \hat{\eta}\hat{\zeta}}^{\epsilon^2} \# \gamma_{yx} \# \gamma_{zx} \rangle = \sum_{n=p_i \pm 1} \sum_{m=p_j \pm 1} \begin{Bmatrix} p_i & p_i & n \\ 1 & 1 & 2 \end{Bmatrix} \begin{Bmatrix} p_j & p_j & m \\ 1 & 1 & 2 \end{Bmatrix} \\ \times \begin{Bmatrix} n & p_i & p_k \\ p_j & m & 1 \end{Bmatrix} \frac{(-1)^{p_k} \vartheta(p_i, p_j, p_k)}{p_k + 1} \cdot \text{Diagram}$$

The last step in the graphical calculation requires more careful consideration. As discussed in [6], when we act on diffeomorphism-invariant states, the spin network remains in its knot class, although the area of the last remaining loop goes to zero. To understand this situation, let us discuss the action of the Hamiltonian from the point of view of diffeomorphism invariance. We start with a state which is diffeomorphism class of spin network and a Hamiltonian, also based on a class of diffeomorphism-invariant smooth loops with ‘‘hands.’’ To perform the action, we introduce a background metric, break the diffeomorphism invariance, and introduce notions of lengths and areas. It is in this noninvariant sense in which we can talk about ‘‘loops of some area shrinking to a fixed point’’ and about ‘‘hands of infinitesimal length.’’ Also, all the formulas we apply from the recoupling theory are based on the ideas of replacing loops by their loop values and recoupling, which are diffeomorphically noninvariant operations. We assume that we can perform these operations as far as we recover at the end of the ‘‘right’’ diffeomorphism class. What we expect at the end is the original spin network attached through two ‘‘hands’’ to a loop which in the nondiffeomorphism limit shrinks to a vertex.

We can choose the attached loop in different way, but we want our choice to be consistent with the operations we perform in a noninvariant fashion. One possible such choice is the attached loop to connect two edges joined at a vertex and then to run along the edges of the original spin network. This means that when the state we are acting on is diffeomorphism invariant, taking the last limit is trivial—the graph does not change. Thus finally we get

$$\langle S, T | \hat{C}_I^{L, \delta, \epsilon} = \frac{3Z}{10\pi} (16\pi l_{Pl}^2)^2 \sum_{i,j} p_i p_j \sum_{n=p_i \pm 1} \sum_{m=p_j \pm 1} \begin{Bmatrix} p_i & p_i & n \\ 1 & 1 & 2 \end{Bmatrix} \\ \times \begin{Bmatrix} p_j & p_j & m \\ 1 & 1 & 2 \end{Bmatrix} \begin{Bmatrix} n & p_i & p_k \\ p_j & m & 1 \end{Bmatrix} \frac{(-1)^{p_k} \vartheta(p_i, p_j, p_k)}{p_k + 1} \cdot \text{Diagram}$$

(34)

where the vertex having the additional edge attached to it is in the I th cube. The state $\langle S, T |$ we acted on is normalized according to the normalization introduced in [12]. If the final states are also to be normalized, we have to introduce some additional factors in Eq. (34). As the old trivalent vertex has been transformed into a new one, and an edge and two new vertices have been added, we get, for the final normalized sum of states,

$$\langle S, T | \hat{C}_I^{L, \delta, \epsilon} = \frac{3Z(16\pi l_{Pl}^2)^2}{10\pi} \\ \times \sum_{i,j} p_i p_j \sum_{n=p_i \pm 1} \sum_{m=p_j \pm 1} \sqrt{\frac{-2\vartheta(p_i, p_j, p_k) \Delta_n \Delta_m}{\vartheta(1, p_i, n) \vartheta(1, p_j, m) \vartheta(n, m, p_k)}} \\ \times \begin{Bmatrix} p_i & p_i & n \\ 1 & 1 & 2 \end{Bmatrix} \begin{Bmatrix} p_j & p_j & m \\ 1 & 1 & 2 \end{Bmatrix} \begin{Bmatrix} n & p_i & p_k \\ p_j & m & 1 \end{Bmatrix} \frac{(-1)^{p_k} \vartheta(p_i, p_j, p_k)}{p_k + 1} \cdot \text{Diagram}$$

(35)

The action of the Hamiltonian constraint \hat{C} as part of the physical Hamiltonian \hat{H} can be described as follows: When the Hamiltonian constraint \hat{C} acts on edges, the action can be interpreted as a diffeomorphism transformation. Thus the Hamiltonian constraint acts nontrivially on diffeomorphism-invariant states only when it acts on the vertices of the spin network. The action on vertices amounts to adding a new edge attached through new trivalent vertices to each pair of edges at each vertex. Each new edge has color 1. Also the colors of the edges connecting the new vertices and the original one change. This change can be explained with the requirement that the new graph is again a spin network. The obtained states are multiplied by finite factors, which, although cumbersome, are straightforward to compute.

V. HAMILTONIAN EIGENSPECTRUM

Let us recall that the Hamiltonian defined through the ‘‘clock’’ field has the form (18):

$$\hat{H} = \lim_{L \rightarrow 0} \sum_I^{\infty} \sqrt{-\lim_{\epsilon \rightarrow 0} \lim_{\delta \rightarrow 0} \hat{C}_I^{L, \delta, \epsilon} + \Lambda \hat{V}_I^2}. \quad (36)$$

To find the eigenspectrum of the Hamiltonian operator, we have to handle in a satisfactory manner the square root in Eq. (36). Since we have not been able to complete this task, we will only describe the directions for future work.

Since both the Hamiltonian constraint and the volume operator in Eq. (36) give nonzero results only when acting on vertices, the above sum reduces to a sum only over the cubes in which there is a vertex. Thus the sum in Eq. (36) becomes finite. Also, all the terms coming from the action on different vertices are independent of each other. This justifies the following strategy for computing the Hamiltonian eigenspectrum: We can use the result from the action of the expression under the square root on vertices—the action of the first term is given by Eq. (35), and the action of the volume piece has been computed for example in [12]. To proceed further we might have to distinguish between the action on bivalent and trivalent vertices, on the one hand, as having zero volume, and the action on higher-valence vertices. In any case we will have to diagonalize the expression (35). The problem is that *a priori* we cannot expect the matrix defined by Eq. (35) to be diagonalizable. Since the expression for the Hamiltonian constraint we start with is a real one, we can assume that there exists an appropriate symmetrization which can make the constraint operator self-adjoint and its matrix symmetric. To make the matrix in the right-hand side of Eq. (35) diagonalizable we could replace it by one-half of the sum of the matrix and its transposed. Then we will have to diagonalize the sum of the Hamiltonian and volume matrices and to take the square root. The result will be an infinite dimensional diagonal matrix with the Hamiltonian eigenvalues as its elements.

VI. CONCLUSION

The action of the Hamiltonian constraint on a spin network state can be described as a transition of the spin net-

works on which the state is based from one knot class of graphs with vertices into another one. In this transition the coloring of certain edges changes, and so the requirements for the graph to be a spin network remain satisfied. At the same time, each new state is multiplied by a factor which carries the appropriate dimensions, contains an arbitrary constant, and also includes the result from the computation in recoupling theory.

In the paper we considered in detail only trivalent vertices, but the generalization to higher valence vertices is straightforward. As discussed in [11,12], any higher-valence vertex can be decomposed into a set of infinitesimally displaced trivalent ones. The analytical calculation we performed did not depend to the valence of the vertex. The difference with the considered case will appear in the graphical evaluation where we again can apply the recoupling theory. It can be shown that as a result in the same way as with the trivalent vertices, edges of color 1 are added, rerouting of the loops through the vertices occurs, and one can compute the corresponding prefactors.

Also, the evaluation presented in the paper can be applied to the q -deformed spin networks [16,18]. In the q -deformed theory, all the formulas we used have their counterparts. Thus in that case one should simply replace the formulas we derived with the corresponding q -deformed versions [15].

As we discussed before, to get rid of the background dependence of the prefactor, we have to know the angle between each pair of tangents, which requires modification of the regularization. Another set of problems occurs when we try to make sense of the square root involved in the definition of the Hamiltonian. There are certain proposals in this direction: One [17] is to use an expansion in inverse powers of Λ and to find an approximation to the square root. Another proposal [7] involves a different procedure, which also allows the square root to be expressed as a series. In any case we have to settle this set of problems before trying to solve for the eigenvalues of the Hamiltonian operator.

ACKNOWLEDGMENTS

This work would be impossible without the numerous discussions I had with Lee Smolin and Carlo Rovelli. I also would like to thank Don Neville and Seth Major for their comments and criticism and the Center for Gravitational Physics and Geometry, where this work was started, for the hospitality.

APPENDIX: BASIC FORMULAS OF THE RECOUPLING THEORY

One of the main results of the recoupling theory of colored knots and links with trivalent vertices [15] is the computation of the Kauffman brackets for different framed spin networks. The framing refers to the fact that in the computations one keeps track of overcrossings and undercrossing. In our work we do not make this distinction, and so we use a simplified version of the recoupling theory; namely, we replace the deformation parameter q by its ‘‘classical’’ value -1 , relevant to our case. As a result, in most of the formulas

from [15], the q -deformed (or quantum) integers are replaced by ordinary ones. We list here the basic formulas, which we use, with the mentioned corrections made. For more details see [15].

The basic relation in this theory expresses the relation between the different ways in which three angular momenta, say, $j_1, j_2,$ and j_3 can couple to form a fourth one, j_4 . The two possible recouplings are related by the formula

$$\left(\begin{array}{c} j_2 \quad j_3 \\ \diagdown \quad \diagup \\ \text{---} J \text{---} \\ \diagup \quad \diagdown \\ j_1 \quad j_4 \end{array} \right) = \sum_I \left\{ \begin{array}{ccc} j_1 & j_2 & I \\ j_3 & j_4 & J \end{array} \right\} \left(\begin{array}{c} j_2 \quad j_3 \\ \diagdown \quad \diagup \\ \text{---} I \text{---} \\ \diagup \quad \diagdown \\ j_1 \quad j_4 \end{array} \right) \tag{A1}$$

where on the right-hand side is the $q-6j$ symbol, as defined in [15] for the value of the deformation parameter q equal to -1 . Again, the dashed line denotes the fact that the recoupling occurs in a region which shrinks to a point; it is not extended in space.

Closed loops which have been shrunk to a point are replaced by their loop value, which is (for a single loop with zero self-linking) equal to -2 . The evaluation of a single unknotted loop with color n is [15]

$$\left(\begin{array}{c} \text{---} n \text{---} \\ \text{---} \square \text{---} \\ \text{---} n \text{---} \end{array} \right) = (-1)^n (n + 1) \equiv \Delta_n. \tag{A2}$$

The small rectangle in the above diagram denotes the antisymmetrization of the n line.

The next graph we consider is the ‘‘bubble’’ diagram. Upon shrinking the ‘‘bubble,’’ this diagram will reduce to a single edge, so that the evaluation will be different from zero only if the colors of both ends of the ‘‘bubble’’ are the same. Thus the ‘‘bubble’’ diagram equals some numerical factor times a single edge. By closing the free ends of the diagram, it is straightforward to show that

$$\left(\begin{array}{c} n \quad a \quad n' \\ \text{---} \text{---} \text{---} \\ \text{---} b \text{---} \end{array} \right) = \delta_{nn'} \frac{(-1)^n \theta(a, b, n)}{n + 1} \left(\begin{array}{c} n \\ \text{---} \end{array} \right) \tag{A3}$$

in which the function $\theta(a, b, n)$ is given, in general, by

$$\theta(m, n, l) = \left(\begin{array}{c} l \\ \text{---} m \text{---} \\ \text{---} n \end{array} \right) = (-1)^{(a+b+c)} \frac{(a + b + c + 1)! a! b! c!}{(a + b)! (b + c)! (a + c)!} \tag{A4}$$

where $a + b = m, a + c = n,$ and $b + c = l$.

A basic element in most of the formulas of the recoupling theory of colored graphs is the $6j$ symbol. It is defined through the so-called tetrahedral net via the relation

$$\left\{ \begin{array}{ccc} a & b & e \\ c & d & f \end{array} \right\} = \frac{(-1)^e (e + 1) \text{Tet} \begin{bmatrix} a & b & e \\ c & d & f \end{bmatrix}}{\vartheta(a, d, e) \vartheta(c, b, e)}. \tag{A5}$$

The tetrahedral net is represented by the diagram

$$= \text{Tet} \begin{bmatrix} a & b & e \\ c & d & f \end{bmatrix}.$$

Upon evaluation, the tetrahedral net yields

$$\text{Tet} \begin{bmatrix} a & b & e \\ c & d & f \end{bmatrix} = \frac{\mathcal{I}}{\mathcal{E}} \sum_{m \leq s \leq M} \frac{(-1)^s (s+1)!}{\prod_i (s-a_i)! \prod_j (b_j-s)!},$$

where

$$a_1 = \frac{1}{2}(a+d+e), \quad b_1 = \frac{1}{2}(b+d+e+f),$$

$$a_2 = \frac{1}{2}(b+c+e), \quad b_2 = \frac{1}{2}(a+c+e+f),$$

$$a_3 = \frac{1}{2}(a+b+f), \quad b_3 = \frac{1}{2}(a+b+c+d),$$

$$a_4 = \frac{1}{4}(c+d+f),$$

$$m = \max\{a_i\}, \quad M = \min\{b_j\},$$

$$\mathcal{E} = a!b!c!d!e!f!, \quad \mathcal{I} = \prod_{ij} (b_j - a_i)!$$

These formulas are sufficient for the computations performed in the paper. In [15], one can find a detailed derivation of all of them.

-
- [1] C. Misner, K. Thorn, and J. Wheeler, *Gravitation* (Freeman, San Francisco, 1973).
- [2] J. Brown and K.uchař, Phys. Rev. D **51**, 5600 (1995).
- [3] T. Schilling, "Bibliography of Publications related to Classical and Quantum Gravity in terms of the Ashtekar Variables," Report No. gr-qc/9409031 (unpublished); C. Beetle and A. Corichi, "Bibliography of Publication Related to Classical and Quantum Gravity in terms of Connection and Loop Variables," Report No. gr-qc/9703044 (unpublished).
- [4] C. Rovelli and L. Smolin, Nucl. Phys. **B331**, 80 (1990).
- [5] L. Smolin, in *Brill Festschrift Proceedings*, edited by B-I Hu and T. Jacobson (Cambridge University Press, Cambridge, England, 1993).
- [6] L. Smolin and C. Rovelli, Phys. Rev. Lett. **72**, 446 (1994).
- [7] C. Rovelli, J. Math. Phys. (N.Y.) **36**, 6529 (1995).
- [8] A. Ashtekar, J. Lewandowski, D. Marolf, J. Mourão, and T. Thiemann, J. Math. Phys. (N.Y.) **36**, 6456 (1995).
- [9] C. Rovelli and L. Smolin, Phys. Rev. D **52**, 5743 (1995).
- [10] J. Baez, *Knots and Quantum Gravity* (Oxford University Press, Oxford, 1994).
- [11] C. Rovelli and L. Smolin, Nucl. Phys. **B442**, 593 (1995).
- [12] R. DePietri and C. Rovelli, Phys. Rev. D **54**, 2664 (1996).
- [13] K.uchař and C. Torre, Phys. Rev. D **43**, 419 (1991).
- [14] M. Blencowe, Nucl. Phys. **B341**, 213 (1990).
- [15] L. Kauffman and S. Lins, *Temperley-Lieb Recoupling Theory and Invariants of 3-Manifolds* (Princeton University Press, Princeton, 1994).
- [16] S. Major and L. Smolin, Nucl. Phys. **B473**, 267 (1996).
- [17] R. Borissov, C. Rovelli, and L. Smolin, "Physical evolution of the spin network states," report, 1994 (unpublished); R. Borissov, C. Rovelli, and L. Smolin, "Dynamics of Non-Perturbative Quantum General Relativity," Report No. CGPG-95/5-1 (unpublished).
- [18] R. Borissov, S. Major, and L. Smolin, Class. Quantum Grav. **13**, 3183 (1996).